

Supporting Information

Circumventing Myeloid-Derived Suppressor Cell-Mediated Immunosuppression Using an Oxygen-Generated and -Economized Nanoplatfom

Huaqin Zuo,^{†,‡} Yuchen Hou,[⊥] Yijun Yu,[†] Zhongqiu Li,[⊥] Hanxiao Liu,[†] Chao Liu,^{,§} Jian He,^{*,□} Leiying Miao,^{*,†}*

[†]Department of Cariology and Endodontics, Nanjing Stomatological Hospital, Medical School of Nanjing University, Nanjing, Jiangsu, 210093, P. R. China.

[‡]Department of Hematology, Northern Jiangsu People's Hospital Affiliated to Yangzhou University, Yangzhou, Jiangsu, 225001, P. R. China.

[§]Department of Orthodontics, Nanjing Stomatological Hospital, Medical School of Nanjing University, Nanjing, Jiangsu, 210093, P. R. China.

[□]Department of Radiology, Nanjing Drum Tower Hospital, The Affiliated Hospital of Nanjing University Medical School, Nanjing University, Nanjing, Jiangsu, 210008, P. R. China.

[⊥]Department of Liver Surgery, RenJi Hospital, School of Medicine, Shanghai Jiao Tong University, Shanghai, 200127, P. R. China.

[⊥]Department of Organ Transplantation, The First Affiliated Hospital of Sun Yat-Sen University, Guangzhou, 510080, P. R. China.

*Corresponding Authors

Chao Liu: dxliuchao@163.com

Jian He: hjxueren@126.com

Leiying Miao: miaoleiying80@163.com

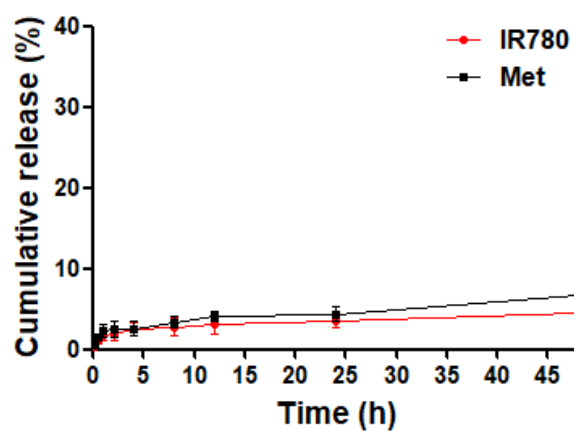


Figure S1. *In vitro* release profile of IR780 and Met from CeO₂@MSNs@IR780/Met nanoparticles in plasma.

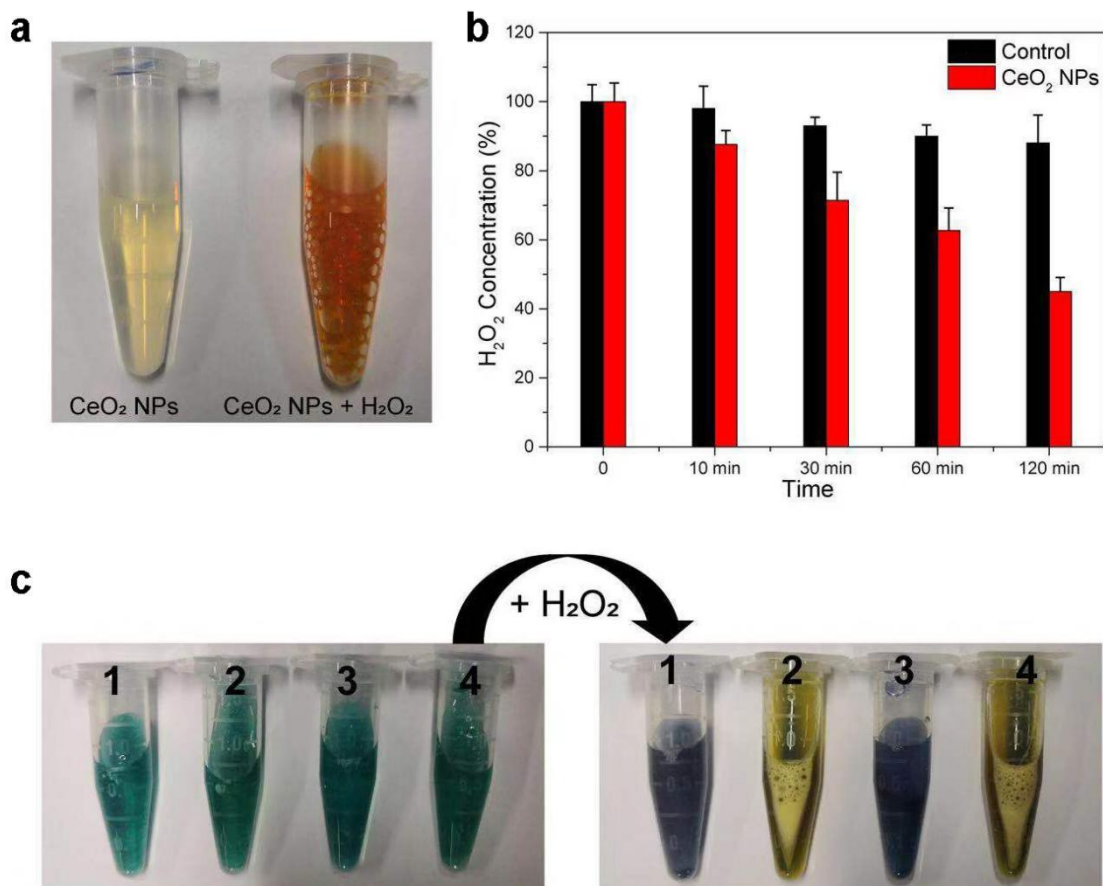


Figure S2. Degradation of H₂O₂ by CeO₂ NPs and the release of O₂. (a) Photographs of CeO₂ NPs before (right) and after (left) reaction with H₂O₂. (b) time-dependent degradation of 10 mM H₂O₂ after reacting with CeO₂ NPs (1 mg/mL) in PBS. (c) Photographs of different nanocompositions of MSNs before (right) and after (left) reaction with H₂O₂, from NO.1 to 4 are MSNs@IR780, CeO₂@MSNs@IR780, MSNs@IR780/Met and CeO₂@MSNs@IR780/Met.

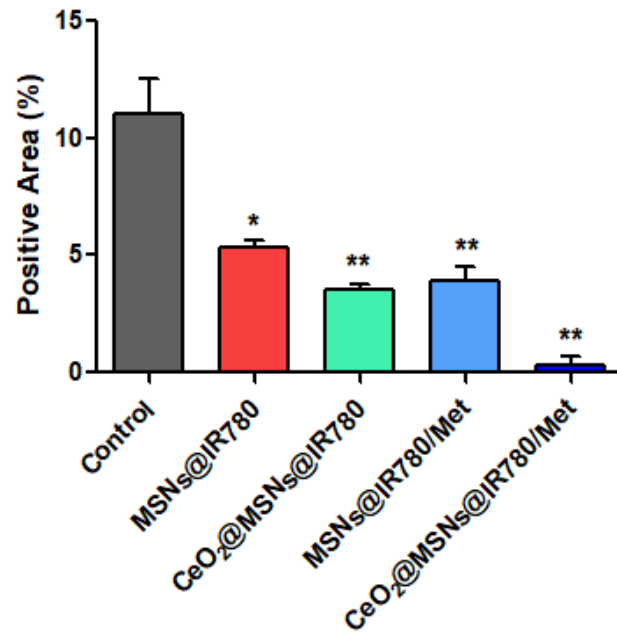


Figure S3. Positive area of Ki-67 in tumor tissues after indicated treatments. * $p < 0.05$, ** $p < 0.01$

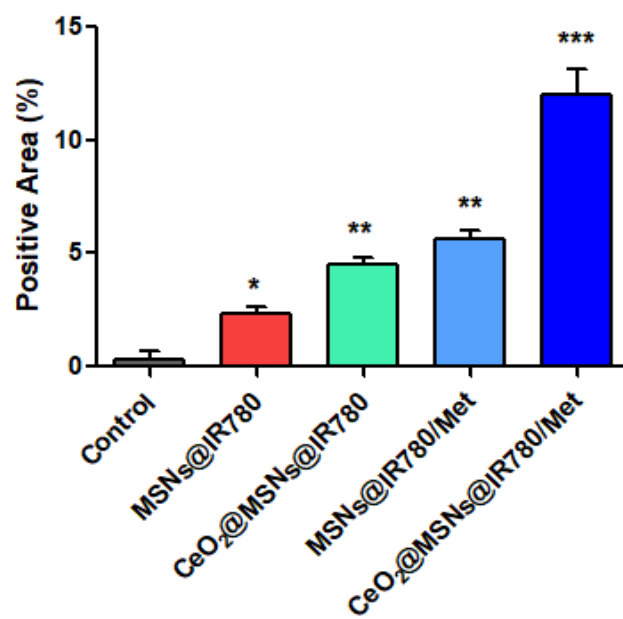


Figure S4. Positive area of TUNEL in tumor tissues after indicated treatments. * $p < 0.05$, ** $p < 0.01$, *** $p < 0.001$

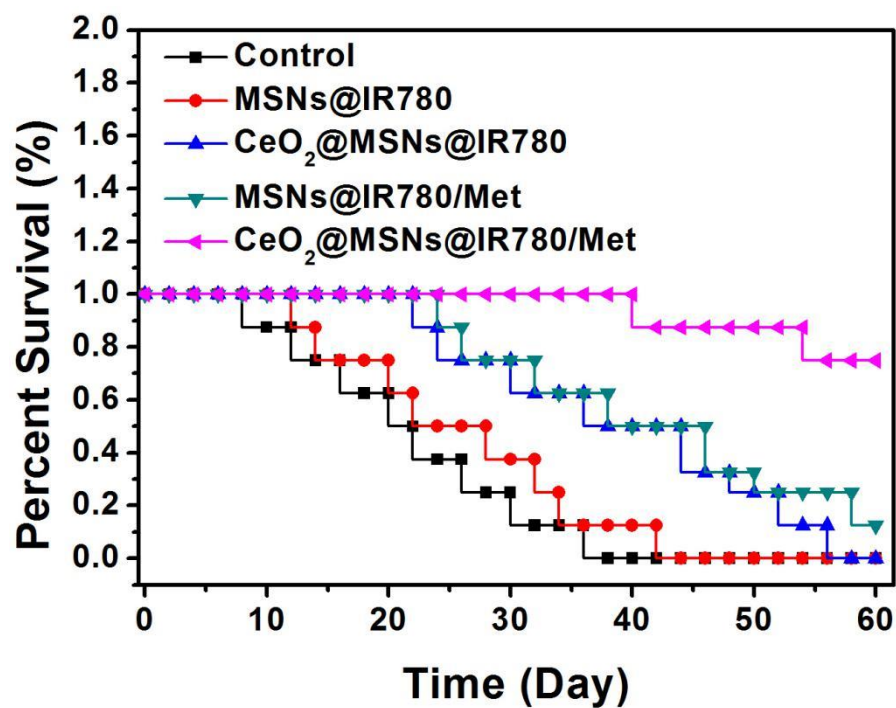


Figure S5. Survival curves of B16F10 tumor-bearing mice that received indicated treatments as displayed. Data were analyzed with Kaplan-Meier method (n = 8).

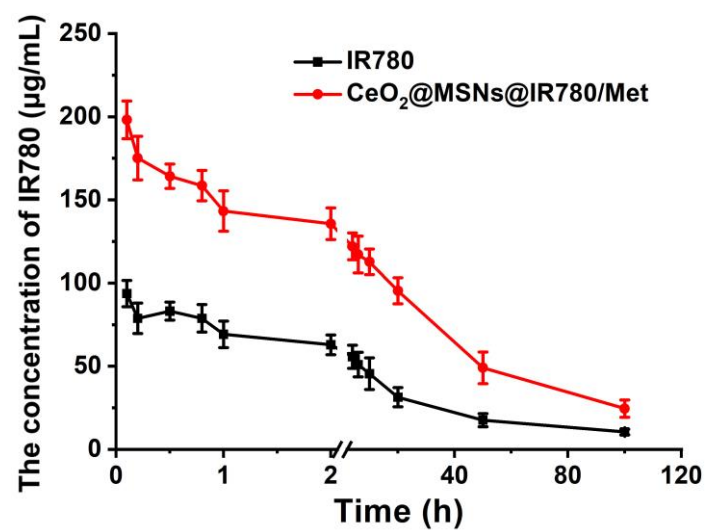


Figure S6. Plasma concentration–time curves of CeO₂@MSNs@IR780/Met in mice after intravenous injection of different IR780 formulations at a dose of 20 mg/kg (n = 5).

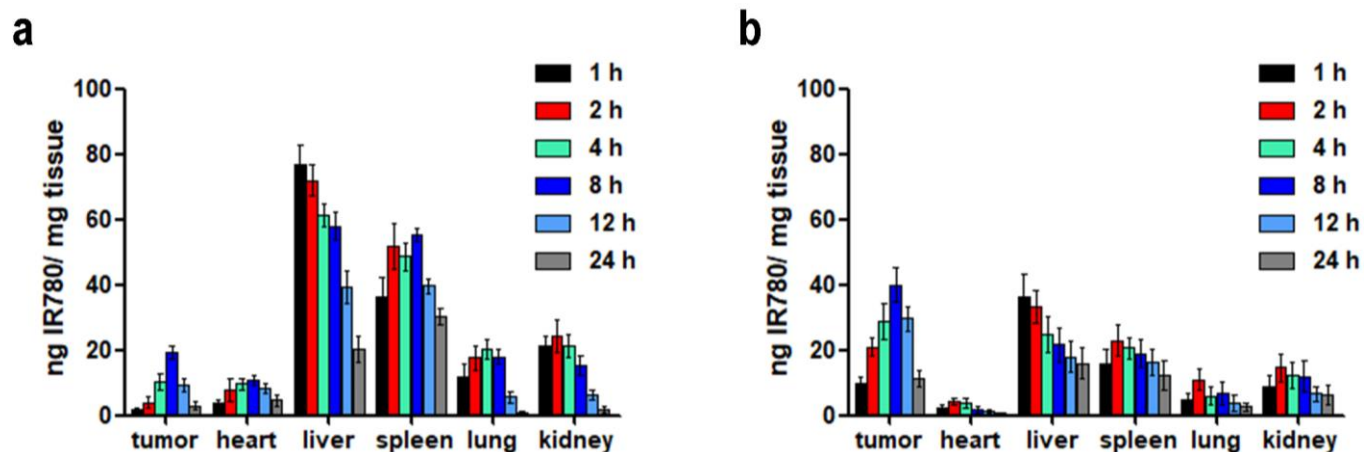


Figure S7. *In vivo* tissue distribution in B16F10 tumor-bearing mice intravenously injected with indicated treatments at different time points (20 mg/kg for IR780). (a) Free IR780. (b) CeO₂@MSNs@IR780/Met (n = 5).

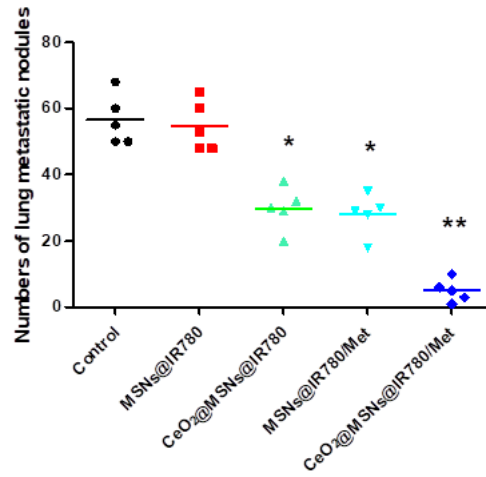


Figure S8. Quantification of the metastatic nodules on the lung surface of mice under different treatments. All results were presented as mean \pm SD (n = 5), * $p < 0.05$, ** $p < 0.01$.

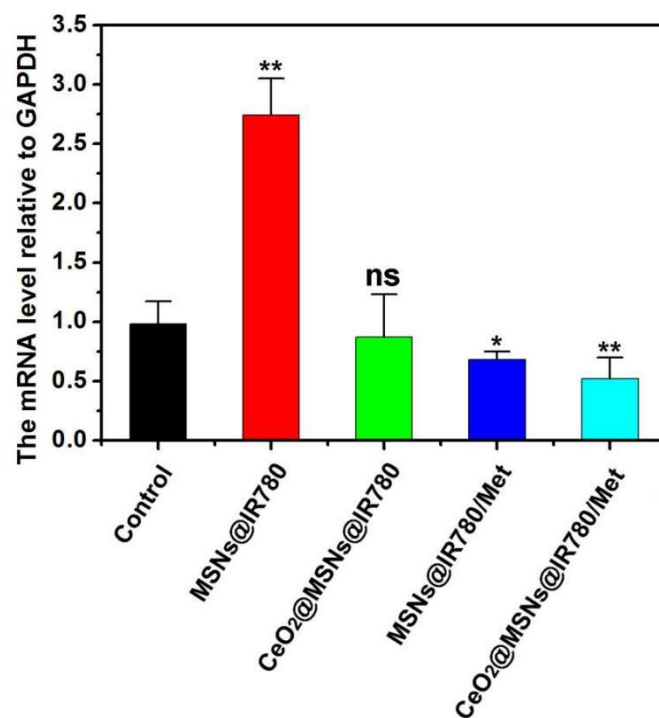


Figure S9. Q-PCR analyzed the mRNA level of HIF- α in tumor tissues from B16F10 tumor-bearing mice subjected to indicated treatments. All results were presented as mean \pm SD ($n = 5$), ns means not significant, * $p < 0.05$, ** $p < 0.01$.

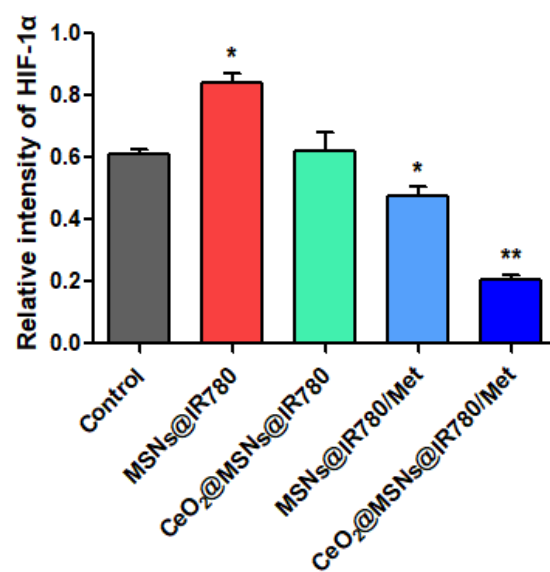


Figure S10. Relative intensity of HIF-1 α protein expression by western blotting. * $p < 0.05$, ** $p < 0.01$

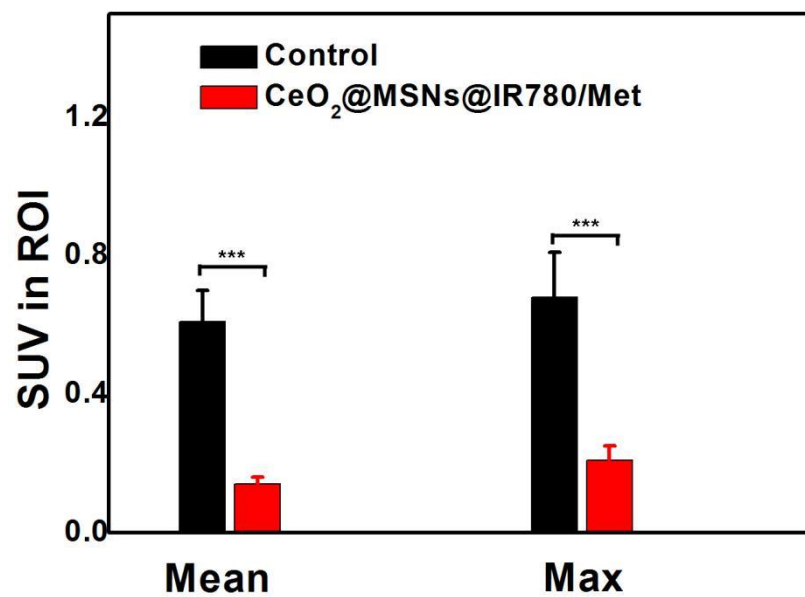


Figure S11. Standardized uptake values (SUVs) in solid tumor regions obtained from in vivo PET images taken at 1 h after the injection of ¹⁸F-MISO. All results were presented as mean ± SD (n = 5), *** *p* < 0.001.

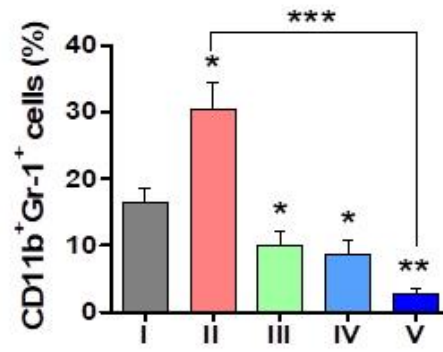


Figure S12. Relative quantification of MDSCs (CD11b⁺Gr-1⁺) in tumor tissues following different treatments (I: Control, II: MSNs@IR780 + laser, III: CeO₂@MSNs@IR780 + laser, IV: MSNs@IR780/Met + laser, V: CeO₂@MSNs@IR780/Met + laser). All results were presented as mean \pm SD (n = 5), * $p < 0.05$, ** $p < 0.01$, *** $p < 0.001$.

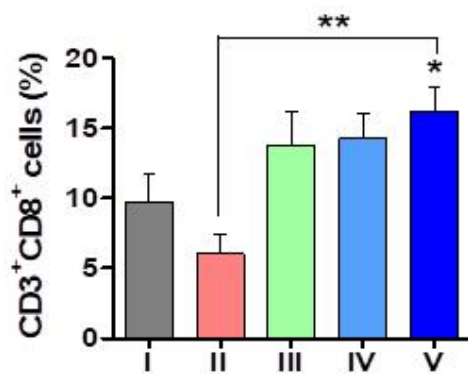


Figure S13. Relative quantification of CTLs (CD3⁺CD8⁺) in tumor tissues following different treatments (I: Control, II: MSNs@IR780 + laser, III: CeO₂@MSNs@IR780 + laser, IV: MSNs@IR780/Met + laser, V: CeO₂@MSNs@IR780/Met + laser). All results were presented as mean \pm SD (n = 5), * p < 0.05, ** p < 0.01.

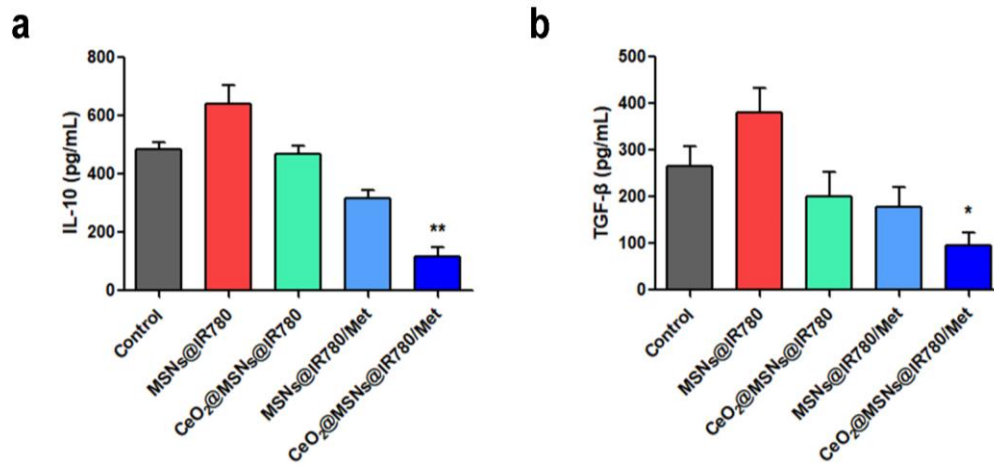


Figure S14. ELISA assay for IL-10 (a) and TGF-β (b). Tumor-infiltrating MDSCs were isolated from the tumors of B16F10 tumor-bearing mice under different treatments and cultured for 24 h. The supernatant was subjected to ELISA analysis. * *p* < 0.05, ** *p* < 0.01.

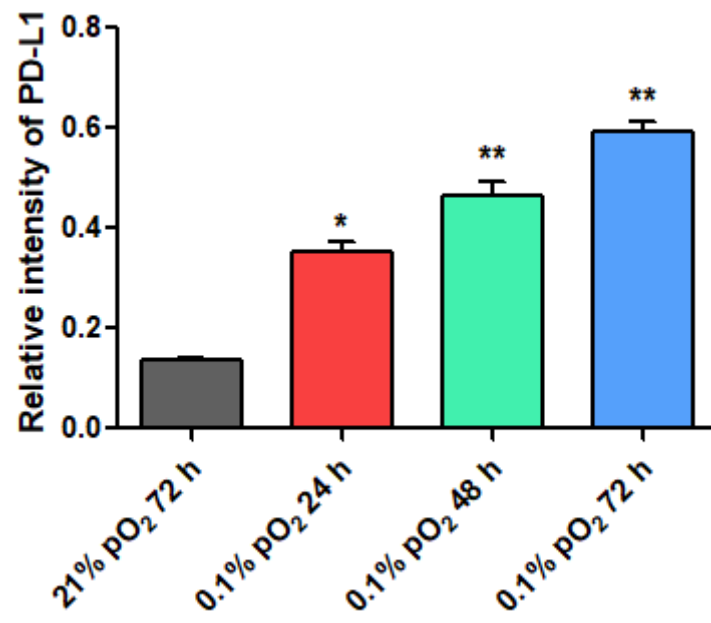


Figure S15. Relative intensity of PD-L1 protein expression by western blotting. * $p < 0.05$, ** $p < 0.01$.

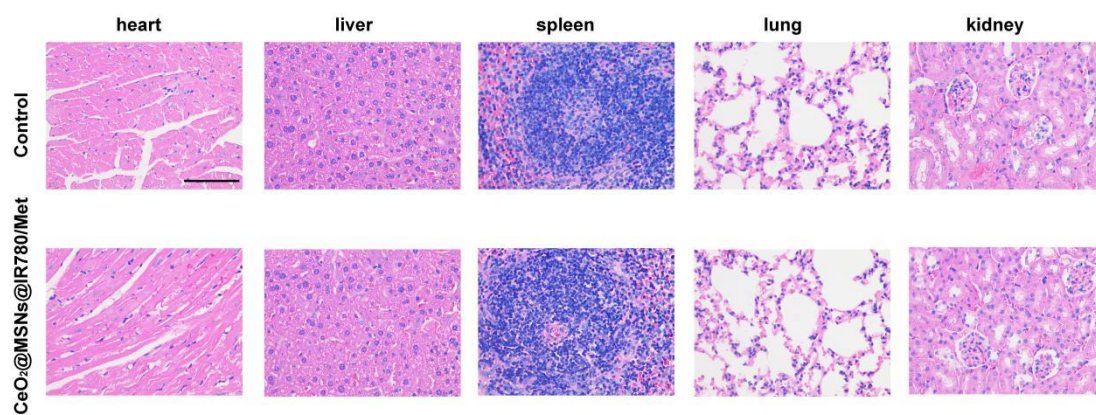


Figure S16. Histology of the mouse organs collected 21 days after the intravenous injection of CeO₂@MSNs@IR780/Met. Scale bar: 100 μ m.